A New Nonsymmetric $As(OH)_3$ Species. Comparison with the Known C_3 Species and Themochemistry at the HF, DFT(B3LYP), MP2, MP4, and CCSD(T) Levels of Theory

Alejandro Ramírez-Solís,*,† Jorge Hernández-Cobos,‡ and Cristina Vargas§

Depto. de Física, Facultad de Ciencias, Universidad Autónoma del Estado de Morelos, Av. Universidad 1001, Cuernavaca, Morelos, 62209 México, Depto. de Biofísica, Centro de Ciencias Físicas, UNAM, Cuernavaca, Morelos, 62209 México, and CINEVESTAV, Unidad Mérida, Mérida, Yucatán, México.

Received: January 8, 2006; In Final Form: March 31, 2006

A new nonsymmetric $As(OH)_3$ species that is more stable than the C_3 structure is found at HF, Density Functional Theory (B3LYP), MP2, MP4 and CCSD(T) levels with the Stuttgart RECP-basis for As and the aug-cc-pvdz/pvtz extended basis sets. Transition state (TS) geometries are close to the C_3 one. Energy differences and interconversion barriers become smaller with increasing inclusion of electronic correlation. However, for MP4 and CCSD(T) descriptions, these differences increase by more than 100% when basis set goes from the AVDZ to AVTZ quality. Zero point energy (ZPE) corrections are essential and have been taken into account at all levels of theory; although this leads to barrier collapse at the B3LYP, MP2, MP4 and CCSD(T) levels, the C_1 isomer remains more stable than the C_3 one. MP2/AVTZ infrared spectra are also given for the C_1 and C_3 isomers as guiding data for future IR studies in the gas phase.

I. Introduction

It is very well established that arsenic is a carcinogen since exposure to arsenic in drinking water is associated with increased risk of skin, kidney, lung, and bladder cancer.[1] Despite a considerable body of literature on arsenic biochemistry,[2] very little is known about the forms of inorganic arsenic present in solution under physiological conditions. Arsenic is a semimetal or metalloid with two biologically important oxidation states, As(V) and As(III), commercially available as the oxyacid arsenic acid (H_3AsO_4) or arsenous acid, also called arsenic trioxide (As_2O_3). Arsenite in water has a pK_a of 9.2, and it has been speculated to exist as $As(OH)_3$ in the hydrated form, though this has never been firmly characterized.[3] The elevated pK_a is relevant for the type of transport system that catalyzes uptake of the pentavalent and trivalent forms of arsenic. Cellular uptake of inorganic arsenate (As(V)) is almost always performed via phosphate transporters.[2] However, it has only recently been recognized that uptake of As(III) is via channels for neutral molecules,[3,4] indicating that $As(OH)_3$ or other related species could be the common form of arsenite in water. Because of the biological consequences, it is very important to understand the solution forms of inorganic arsenic compounds. Therefore, one of us participated in a theoretical and experimental characterization of the coordination environment of hydrated As compounds to provide a basic structural understanding of how the metalloid exists in solution.[5] Two complementary methods were used to identify the coordination environment of arsenite in water. X-ray absorption spectroscopy (XAS) was used to determine the nearest neighbor coordination environment of arsenite under a variety of solution conditions. XAS results were compared to a structural database of arsenite compounds to identify probable coordination geometries for the metalloid in solution. In that study, cluster quantum chemical studies (including only up to three water molecules) were carried out to obtain a preliminary understanding of how As(III)-O interactions govern the solution forms of hydrated arsenic; these results point to neutral $As(OH)_3$ as the most stable structure existing in solution at neutral pH and it seems to be active metalloid form which is subject to cellular uptake, causing all the previously mentioned biological consequences. Thus, no ionic As transport seems to be involved in the uptake. When combined, these investigations provide a basic understanding of the molecular structure of solvated arsenite, with direct implications into the reactive form of the metalloid that gets imported by cells, causing arsenic toxicity.

To make a better description of the structure of $As(OH)_3$ solvated in water, we decided to apply the well-established methodology of the CCF−Cuernavaca group[6−8] to study molecular systems in solution, based on molecular dynamics (MD) and Monte Carlo (MC) simulations using many-body classical potentials parametrized from accurate quantum chemical MP2 surfaces. During the iterative self-consistent procedure used to obtain an increasingly accurate description of the two- [$As(OH)_3-H_2O$] and three-body [$As(OH)_3-(H_2O)_2$] potential terms, we found that another less symmetrical (C_1) stable $As(OH)_3$ structure existed. We report here the new bare optimized structure and its associated energy barrier to the symmetric C_3 structure, obtained through HF, DFT(B3LYP), MP2, MP4, and CCSD(T) calculations. The vibrational spectra have also been calculated to characterize geometries of the global C_1 and local C_3 minima as well as the transition state.

Finally, we point out that no implications of the existence of this new isomer are envisaged in relation to the As−O coordination environment in solution, mainly because the interaction energies with the solvating environment are much larger than the minute energy differences found between these two isomers and, second, due to the larger conformational changes of $As(OH)_3$ induced by solvation than those involved in the C_1-C_3 interconversion.

* Corresponding author: alex@servm.fc.uaem.mx.
† Depto. de Física, Facultad de Ciencias. Universidad Autónoma del Estado de Morelos.
‡ Depto de Biofísica, Centro de Ciencias Físicas, UNAM.
§ CINEVESTAV, Unidad Mérida.

10.1021/jp0601365 CCC: $33.50
Published on Web 05/26/2006

TABLE 1: B3LYP/AVDZ and MP2/AVDZ Optimized Geometries,[a] Where the Main Parameters Are Also Given for the MP2 Optimized Structures with the AVTZ Basis Sets, with Distances in Angstroms and Angles in Degrees

	B3LYP/AVDZ			MP2(fc)/AVDZ,AVTZ		
$As(OH)_3$	C_1	TS	C_3	C_1	TS	C_3
As−O distances	1.826	1.820	1.813	1.803, 1.763	1.812, 1.812	1.814, 1.775
	1.800	1.811	1.813	1.797, 1.757	1.805, 1.806	1.814, 1.775
	1.796	1.806	1.813	1.828, 1.788	1.823, 1.824	1.814, 1.775
O−H distances	0.967	0.969	0.970	0.973, 0.966	0.973, 0.973	0.973, 0.966
	0.969	0.969	0.970	0.974, 0.966	0.973,0.974	0.973,0.966
	0.970	0.970	0.970	0.970, 0.964	0.972, 0.972	0.973, 0.966
O−As−O angles	99.611	97.975	97.355	101.62, 101.806	99.685, 99.686	97.074, 97.770
	90.856	94.950	97.338	99.028, 99.356	97.686, 97.686	97.074, 97.770
	100.888	99.225	97.365	90.533, 91.343	94.105, 94.105	97.074, 97.770
As−O−H angles	112.777	110.288	109.930	111.41, 112.505	109.99, 109.988	108.447, 109.723
	112.675	111.005	109.941	108.95, 110.438	107.92, 107.922	108.447, 109.723
	110.156	109.374	109.925	111.60, 112.240	108.93, 108.929	108.447, 109.723
dihedral O−As−O−H	79.094	15.555	-1.796	-41.549	-17.051	-2.38
	-179.712	115.611	96.654	50.876	78.475	95.69
	52.074	82.942	96.523	89.342	90.857	95.69
	-40.677	-13.433	-1.903	-9.988	-7.670	2.38
	-5.100	-5.116	-1.997	70.385	19.318	2.38
	94.856	93.809	96.444	172.245	119.681	95.69

[a] The optimized geometries are available upon request in **Z**-matrix format.

II. Method: Quantum Chemical Calculations

The ab initio Hartree−Fock, MP2, MP4(SDQ), CCSD(T) and density functional theory (DFT) based calculations were done for the classic C_3 and for the new C_1 $As(OH)_3$ structures. All geometry optimizations are fully unconstrained and used the energy-adjusted Stuttgart relativistic effective core potential (RECP) for As, along with its optimized Gaussian basis set [As].[9] This RECP includes all the main scalar relativistic effects (Darwin and mass−velocity) which are important for heavy elements such as As. It uses a nickel-type core and leaves five active valence electrons. For oxygen and hydrogen, the augmented correlation-consistent polarized valence double- and triple-ζ (aug-cc-pvdz or AVDZ, aug-cc-pvtz or AVTZ) basis sets of Dunning[10] were used. For a balanced description the calculations using the larger AVTZ basis, the As basis was augmented with a set of diffuse s and p orbitals (exponents 0.11 and 0.025 respectively). For the DFT calculations the B3LYP exchange-correlation functional was used as programmed in the Gaussian98 code.[11] The transition states (TS) linking the C_1 and C_3 geometries were found using the reactants−products quasi-synchronous transit (QST2) algorithm as programmed in the G98 code;[11] the TSs were further characterized by vibrational analysis showing a single imaginary frequency at all levels of theory.

For the higher correlated ab initio methods, MP2, MP4(SDQ), and CCSD(T), the zero-point energy corrections were obtained using the MP2 harmonic vibrational frequencies for both basis sets.

III. Results and Discussion

A. General Information. We start by pointing out that, besides the basic interest in a new and more stable isomer for the molecule, the structure of the naked $As(OH)_3$ species is also important because slight changes in the intramolecular geometrical parameters could, in principle, induce qualitative solvation effects due to the (otherwise unlikely or forbidden) possibility to form networks of hydrogen bonds with the water molecules in the first solvation shell. However, we shall not address this last issue here since this would require, as will be shown later, a temperature-dependent (dynamic) and microsolvation-controlled study, which is out of the scope of the present work. Therefore, we will present only static results comparing the new C_1 with the previously known C_3 structure.

B. Geometries and Vibrational Spectra. Table 1 shows the As−O distances, O−As−O angles, and O−As−O−O dihedrals of the optimized geometries of the new C_1, the previously known C_3 species and the corresponding TS at the HF, B3LYP, and MP2 levels of theory using the AVTZ basis sets. The optimized MP2/AVTZ structures for the C_3, TS, and C_1 species are pictorially depicted in Figure 1, parts a, b, and c, respectively. For the TS structure (Figure 1b), the atomic displacements of the imaginary interconversion mode are pictorially shown with the corresponding arrow lengths. It should be noted that for the C_1 isomers, the As−O distances show three slightly different As−O bonds at 1.757, 1.763, and 1.788 Å. Overall, the main feature of the C_1 isomers (at all levels of theory) is that one of the OH goes slightly below and inside the O−As−O umbrella, as compared with the symmetric C_3 one.

The transition states, although slightly unsymmetrical, are actually much closer to the C_3 symmetric stable isomer and, following Hammond's principle, this fact has energetic implications that are verified quantitatively in Table 2.

Although not presented here the HF-optimized geometries are quite well described if one uses the MP2 structures as reference; however, it is somewhat surprising that electronic correlation has little effect on the geometrical parameters governing the stability of these species.

When using a larger AVTZ basis (and including the diffuse s and p orbitals already mentioned for As), the most important geometry changes arise for the As−O distances of the stable C_1 and C_3 structures, all getting shorter roughly by 0.04 Å at the MP2 levels; note, however, that the MP2 optimized TS geometry remains practically unchanged when going from the AVDZ to the AVTZ basis sets.

The calculated MP2 vibrational spectra for both isomers and the transition state are given in Table 3 for both basis sets used. Note the rather small (121 or 116 cm^{-1}) imaginary frequency at the TS geometry associated with the interconversion mode; the corresponding HF and B3LYP imaginary frequencies are close to this value (148 and 138 cm^{-1}, respectively) with the AVDZ basis set. The largest changes in ZPE when going from the AVDZ to the AVTZ basis are found for the C_1 and TS

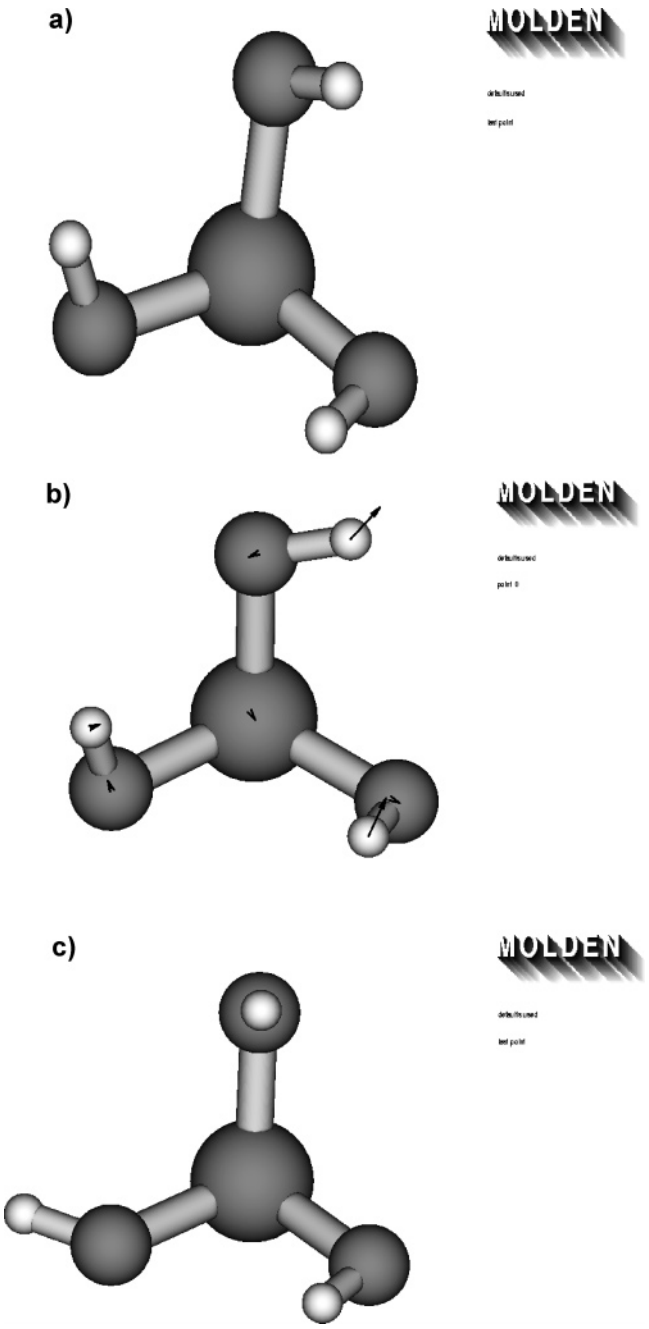

Figure 1. MP2/AVTZ optimized structures for the C_3 species (a), the transition state (b), and the C_1 (c) species**.** Arrows on the transition state show the atomic displacements of the imaginary frequency corresponding to the interconversion mode**.**

structures, while for the perfectly symmetric C_3 species, the ZPE correction with both basis sets is almost identical.

In Figure 2, we show the theoretical infrared spectra (with Lorentzian convolution) for the C_1 (a) and the C_3 (b) species, respectively, that can perhaps be used as reference data to compare with experimental IR results obtained in the gas phase in the near future.

C. Relative Energetics between the C_1 and C_3 Isomers. Since the energy barriers were found to decrease with higher correlated methods with the AVDZ basis set, we deemed necessary to make a systematic study using even more sophistacted methods, including a larger fraction of dynamic correlation energies and with a larger basis set, to verify that the C_1 structure actually remains the absolute minimum in the potential energy surface of $As(OH)_3$. Thus, the relative energies of the

TABLE 2: Thermochemistry at Different Levels of Theory Using the RECP(As)/AVDZ and AVTZ Basis Sets, Where Energy Differences Are Given with Respect to the Lowest Energy Structure (C_1) with and without ZPE Corrections in kcal/mol[a]

$As(OH)_3$ structure	Hartree−Fock	B3LYP	MP2	MP4(SDQ)[b]	CCSD(T)[b]
		Transition State			
AVDZ	0.725	0.525	0.353	0.358	0.329
with ZPE	0.372	0.253	−0.037	−0.032	−0.061
AVTZ	1.181	0.763	0.794	0.825	0.721
with ZPE	0.772	0.433[c]	0.434[c]	0.465[c]	0.361[c]
		C_3			
AVDZ	0.691	0.498	0.287	0.289	0.254
with ZPE	0.411	0.292	0.161	0.163	0.128
AVTZ	1.153	0.750	0.775	0.805	0.694
with ZPE	0.743	0.510	0.465	0.495	0.384

[a] As reference, the optimized MP2/AVTZ energy for the C_1 isomer is −233.387566 au. [b] Single-point calculations using the MP2 optimized geometries; ZPE-corrections from the MP2 vibrational frequencies used for the MP4(SDQ) and CCSD(T) corrected energies. [c] Note the disappearance of the interconversion barriers with the inclusion of the ZPE correction.

TABLE 3: Vibrational Spectra for Both Stable Species of $As(OH)_3$ and the Corresponding Transition State at the MP2/AVDZ and MP2/AVTZ Levels, Where First and Second Columns Respectively Stand for Each Structure and Frequencies are given in cm^{-1} and ZPE Corrections in kcal/mol

C_1	TS	C_3
132.38, 150,78	−121.12, −115.88	137.37, 121.1
193.22, 220.50	208.56, 203.90	137.37, 121.1
268.06, 279.343	283.69, 290.66	294.97, 304.83
299.57, 312.34	297.20, 306.25	301.49, 304.84
341.46, 346.23	322.00, 317.23	301.49, 309.49
377.22, 389.67	414.30, 408.53	421.52, 407.04
629.16, 638.64	628.12, 641.78	635.13, 647.69
654.79, 670.49	642.86, 653.48	635.13, 647.70
679.27, 699.67	672.85, 686.29	670.71, 684.71
941.59, 910.31	935.99, 905.87	953.96, 916.19
960.54, 920.70	959.85, 923.11	953.96, 916.20
1003.15, 970.04	984.89, 943.25	975.73, 938.39
3756.2, 3799.24	3752.27, 3799.35	3763.16, 3805.32
3768.3, 3805.18	3767.83, 3809.36	3766.02, 3809.21
3803.0, 3842.03	3783.53, 3818.30	3766.02, 3809.21
ZPE	ZPE	ZPE
25.45, 25.67	25.06, 25.31	25.33,25.36

symmetric and nonsymmetric structures as well as the energy barriers (with and without ZPE corrections) are shown in Table 2 at the HF, B3LYP, MP2, MP4(SDQ), and CCSD(T) levels, for both basis sets used.

An interesting point comes from the observation (see Table 3) that, since the passage from the C_3 to the C_1 structures leads to splitting of degenerate frequencies, some of them becoming larger and some becoming smaller, overall, the ZPE contributions of both isomers and the TS practically cancel out, but not quite. However, given the extremely small electronic energy differences, the also small ZPE differences play crucial roles, making the energy barriers even smaller, at all levels of theory. The most dramatic effects are found at the MP2, MP4(SDQ), and CCSD(T) levels, where the ZPE(MP2)-corrected barriers disappear, with both basis sets.

Note that while the ZPE corrections are increased by around 0.25 kcal/mol for the C_1 and the TS structures when improving the basis set quality, for the symmetric C_3 isomer the change is eight times smaller (0.03 kcal/mol).

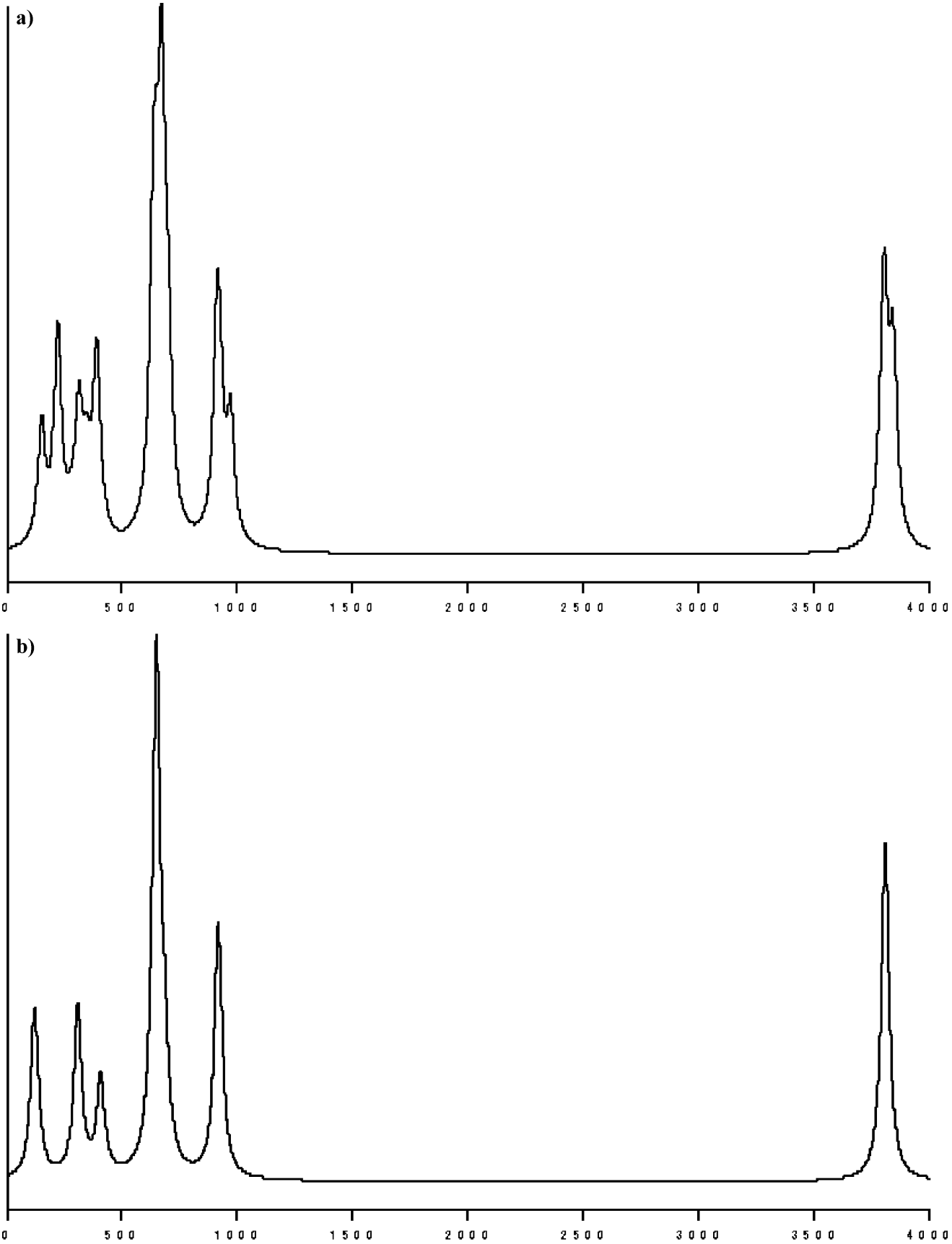

Figure 2. IR calculated at the MP2/AVTZ level: (a) for the C_1 species; (b) for the C_3 species. Frequency is given in wavenumbers.

It is noteworthy that, by a remarkable cancellation of errors, the HF energy differences using the smaller AVDZ basis set (needing less than 3 min of CPU time) are actually very close to the "best estimates" provided by the CCSD(T) values obtained with the much larger AVTZ basis and requiring more than 23 CPU hours.

An interesting fact is that both MP4(SDQ) energy differences are slightly overestimated when compared with the CCSD(T) corresponding values; this is observed with both basis sets. MP2 values are actually closer to the CCSD(T) ones due to cancellation errors of the missing energetic contributions from higher-than-double excitations in the MP2 scheme.

It is clear that such small energy differences make the experimental observation of two structurally distinct isomers a very difficult task and a refined experimental vibrational study in the gas phase is required. The inclusion of ZPE effects are essential given the minute energy differences involved. Note that since our "best" ZPE-uncorrected energy barrier is only 0.72 kcal/mol at the CCSD(T)/AVTZ level, even thermal fluctuations at temperatures as low as 300 K allow very rapid interconversion processes through vibrational excitation between these isomers. Also it should be noted that, at all levels of theory used here, the flatness of the potential energy surface around the three critical points (the C_1, C_3 minima and the transition state) poses problems for a truly accurate description, since nonnegligible contributions from the anharmonic terms may actually lead to vibronic couplings that link the "separate" wells of the C_1 and the totally symmetric C_3 structures. Further work is thus needed to obtain a deeper understanding of the role of these higher order vibrational contributions to the corresponding enthalpies.

IV. Conclusions

Since hydrated arsenic is most likely the initial form of the metalloid absorbed by cells, it has become crucial to understand the structural aspects of arsenic in water. A detailed theoretical characterization of the coordination environment of hydrated As (through the development of many-body interaction potentials) has accidentally led to the discovery of another lower energy nonsymmetric structure for the naked $As(OH)_3$ species. This structure is now being used as the lowest energy reference for the construction of the two- and three-body interaction potentials with water currently developed to perform Monte Carlo and molecular dynamics simulations of this As species in solution at neutral pH. We have characterized as true minima the C_1 (global) and the C_3 (local) isomers and determined the geometry of the transition state linking these structures through very accurate quantum chemical calculations including electronic correlation effects up to the CCSD(T) level with the large augmented correlation-consistent polarized valence triple-ζ basis sets of Dunning. In all cases the single-reference wave function has been found to be adequate for later correlated descriptions.

The zero-point energy corrections are found to play essential roles and their importance have been assessed through the use of different basis sets and increasing sophistication in the electronic correlation treatments. At the MP4 and CCSD(T) levels the MP2 vibrational spectra were used to include the ZPE corrections; although this leads to barrier collapse with both basis sets, the C_1 isomer still remains more stable than the C_3 symmetric one.

The very small enthalpy difference and energy barrier for interconversion between the classic C_3 and the new C_1 structures undoubtedly make the experimental detection of these distinct species a very difficult task. We estimate that the C_1 to C_3 interconversion barrier can be surmounted at temperatures roughly above 350K, but even below that threshold the extremely small purely enthalpic difference between the C_1 and C_3 species will lead to almost equivalent populations of both isomers in the gas phase at very low dilution (neglecting the entropic contribution from eventual clustering/aggregation processes). We provide theoretical infrared spectra for these species in the hope that some experimental evidence of the existence of the nonsymmetric species can be found in low-temperature gas-phase experiments in the near future.

Finally, it is clear that the existence of this new nonsymmetric structure for $As(OH)_3$ allows the possibility that similar nonsymmetric structures could exist also for the isovalent $N(OH)_3$, $P(OH)_3$, $Sb(OH)_3$. and $Bi(OH)_3$ molecules. Work is under way to study the relative stability of these species.[12]

The discovery of this less symmetric species might have unexpected effects on the crystallographic properties of the solid phases of these compounds through the possible existence of symmetry reductions in the actual space groups that are generally acknowledged as the true groups of the corresponding molecular crystals; this requires a detailed study,[13] which is out of the scope of the present work.

Acknowledgment. A.R.-S. acknowledges support from CONACYT Project 45986-E and FOMES2000-SEP through the project "Cómputo científico" for unlimited CPU time on the IBM-p690 supercomputer at UAEM.

References and Notes

(1) Smith, A. H.; Hopenhayn-Rich, C.; Bates, M. N.; Goeden, H. M.; Hertz-Picciotto, I.; Duggan, H. M.; Wood, R.; Kosnett, M. J.; Smith, M. T. *Environ. Health Perspect.* **1992**, *97*, 259.

(2) Rosen, B. P. *FEBS Lett.* **2002**, *529*, 86.

(3) Liu, Z.; Shen, J.; Carbrey, J. M.; Mukhopadhyay, R.; Agre, P.; Rosen, B. P. *Proc. Natl. Acad. Sci. U.S.A.* **2002**, *99*, 6053.

(4) Sanders, O. I.; Rensing, C.; Kuroda, M.; Mitra, B.; Rosen, B. P. *J. Bacteriol.* **1997**, *179*, 3365.

(5) Ramírez-Solís, A.; Mukopadhyay, R.; Rosen. B. P.; Stemmler, T. *Inorg. Chem.* **2004**, *43*, 2954.

(6) Saint-Martín, H.; Hernández-Cobos, J.; Bernal-Uruchurtu, M. I.; Ortega-Blake, I.; Berendsen, H. J. C. *J. Chem. Phys.* **2000**, *113*, 10899 and references therein.

(7) Hernández-Cobos, J.; Saint-Martín, H.; Ortega, I. *J. Chem. Phys.* **2005**, *122*, 224509.

(8) Hernández-Cobos, J.; Saint-Martín, H.; Mackie, A. D.; Vega, L. F.; Ortega-Blake, I. *J. Chem. Phys.* **2005**, *123*, 044506.

(9) Bergner, A.; Dolg, M.; Kuechle, W.; Stoll, H.; Preuss, H. *Mol. Phys.* **1993**, *80*, 1431.

(10) Dunning, T. H., Jr. *J. Chem. Phys.* **1989**, *90*, 1007. Kendall, R. A.; Dunning, T. H., Jr.; Harrison, R. J. *J. Chem. Phys.* **1992**, *96*, 6796.

(11) Frisch, M. J.; Trucks, G. W.; Schlegel, H. B.; Scuseria, G. E.; Robb, M. A.; Cheeseman, J. R.; Zakrzewski, V. G.; Montgomery, J.; J. A.; Stratmann, R. E.; Burant, J. C.; Dapprich, S.; Millam, J. M.; Daniels, A. D.; Kudin, K. N.; Strain, M. C.; Farkas, O.; Tomasi, J.; Barone, V.; Cossi, M.; Cammi, R.; Mennucci, B.; Pomelli, C.; Adamo, C.; Clifford, S.; Ochterski, J.; Petersson, G. A.; Ayala, P. Y.; Cui, Q.; Morokuma, K.; Rega, N.; Salvador, P.; Dannenberg, J. J.; Malick, D. K.; Rabuck, A. D.; Raghavachari, K.; Foresman, J. B.; Cioslowski, J.; Ortiz, J. V.; Baboul, A. G.; Stefanov, B. B.; Liu, G.; Liashenko, A.; Piskorz, P.; Komaromi, I.; Gomperts, R.; Martin, R. L.; Fox, D. J.; Keith, T.; Al-Laham, M. A.; Peng, C. Y.; Nanayakkara, A.; Challacombe, M.; Gill, P. M. W.; Johnson, B.; Chen, W.; Wong, M. W.; Andrés, J. L.; González, C.; Head-Gordon, M.; Replogle, E. S.; Pople, J. A. Gaussian 98 A.11.3; Gaussian Inc.: Pittsburgh, PA, 2002.

(12) Ramírez-Solís, A.; Maron, L. To be published.

(13) Ramírez-Solís, A.; Zicovich-Wilson, C. Unpublished work.